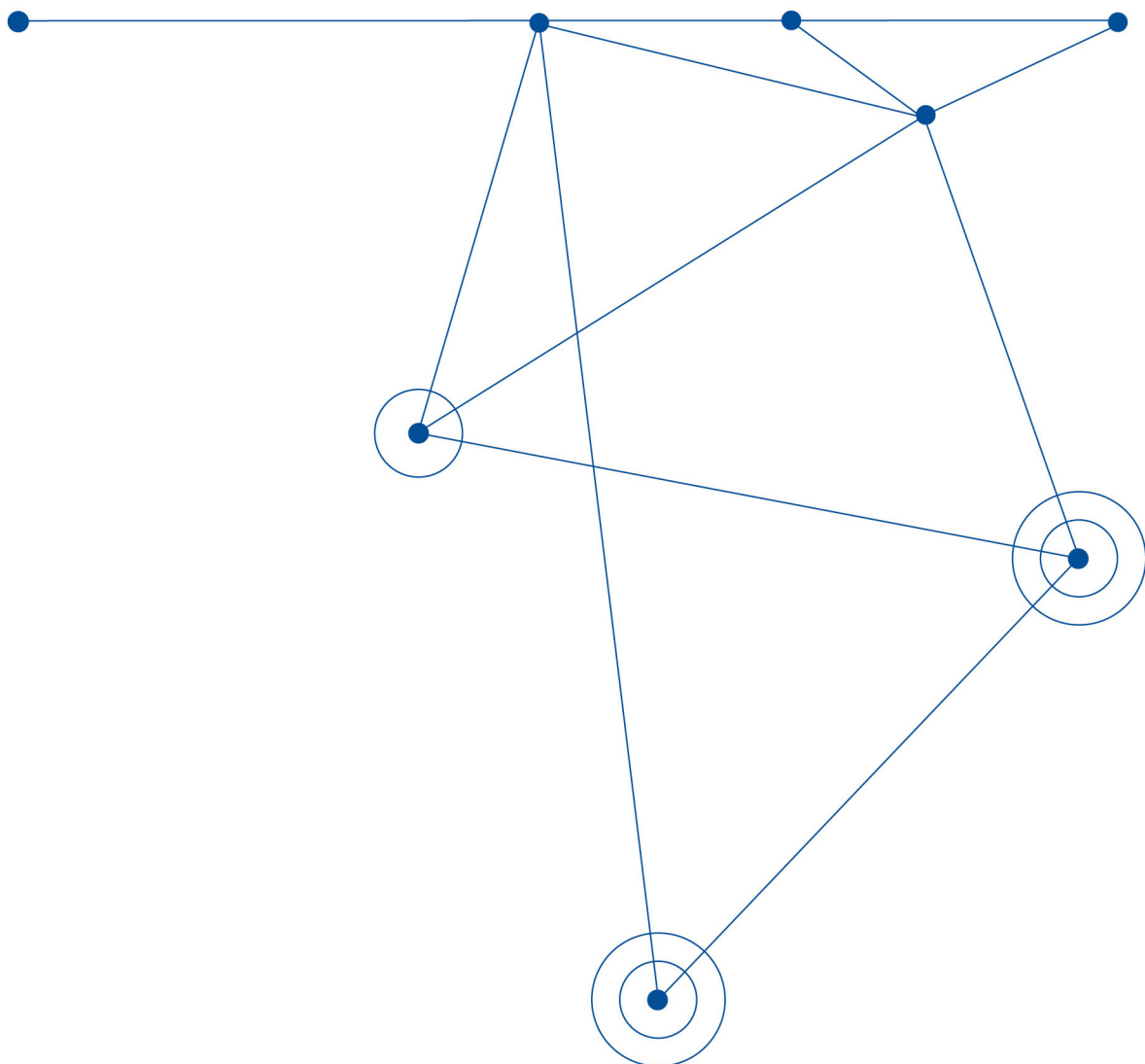


## Measurements in the wake of an undulating membrane tidal energy converter

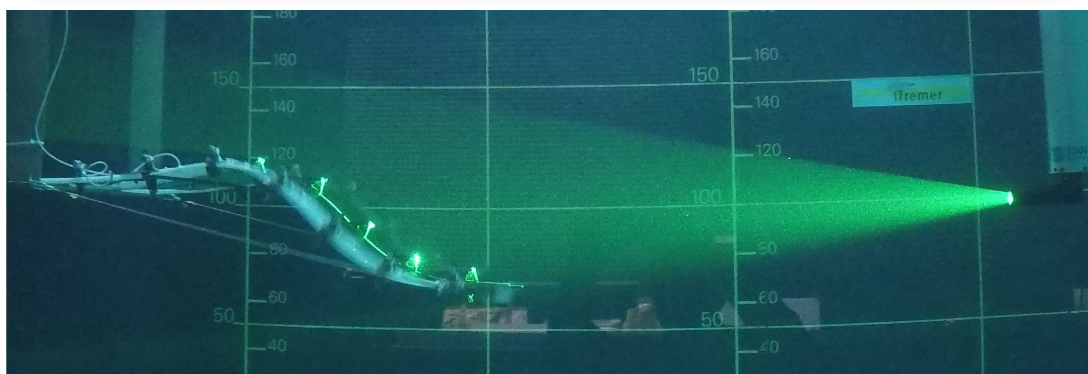
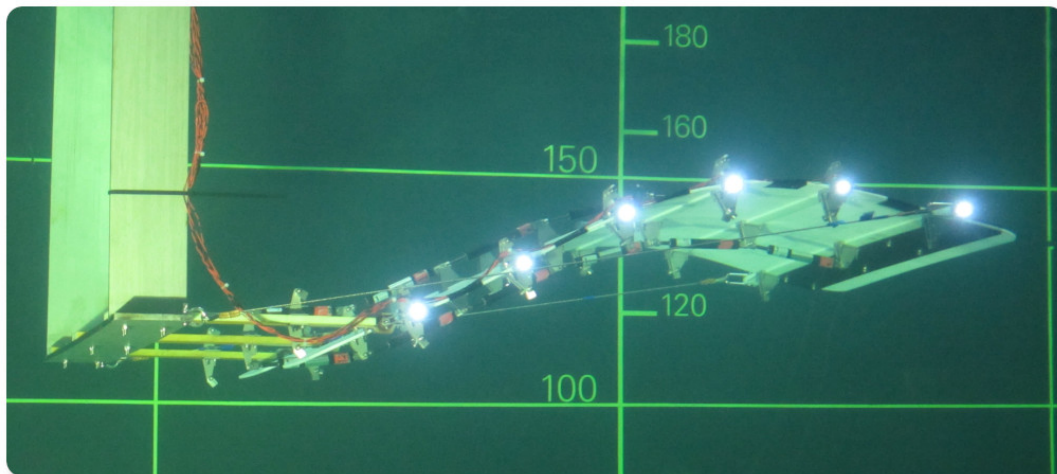
PIV database





# Measurements in the wake of an undulating membrane tidal energy converter

## PIV database



## Fiche documentaire

<b>Titre du rapport :</b> Measurements in the wake of an undulating membrane tidal energy converter - PIV database	
<b>Référence interne :</b> 05CSMBL20  <b>Diffusion :</b> <input checked="" type="checkbox"/> libre (internet)  <input type="checkbox"/> restreinte (internet) - date de levée d'embargo :  <input type="checkbox"/> interdite (confidentielle) - date de levée de confidentialité :	<b>Date de publication :</b> 06.04.2020 <b>Version :</b> 1.0.0  <b>Référence de l'illustration de couverture :</b> Crédit photo/titre/date  <b>Langue(s) :</b> Français - Anglais
<b>Résumé / Abstract :</b> The tidal energy converter studied here is based on the fluid-structure interactions that occur between a flexible membrane and an axial flow, resulting in an undulating motion that can be used to harvest energy. Its wake is experimentally characterized from two-dimensional Particle Image Velocimetry (PIV) measurements. PIV is synchronized with a motion tracking system that gives information on trajectory and power conversion. Wake measurement gives access to velocity deficit, turbulence intensity and vorticity. Three configurations are tested in order to identify the influence of the main adjustment parameters.	
<b>Mots clés / Key words :</b> Marine Renewable Energy, Tidal Energy, Undulation, Power Take-Off, Wake characteristics, Flume tank	
<b>Comment citer ce document :</b>	
<b>Disponibilité des données de recherche :</b>	
<b>DOI :</b> <a href="https://doi.org/">https://doi.org/</a>	

<b>Commanditaire du rapport :</b>	
<b>Nom / référence du contrat :</b> <input type="checkbox"/> Rapport intermédiaire <input checked="" type="checkbox"/> Rapport définitif	
<b>Projets dans lesquels ce rapport s'inscrit :</b>	
<b>Auteur(s) / Adresse mail</b> Träsch Martin / <a href="mailto:mareutin@gmail.com">mareutin@gmail.com</a> Gaurier Benoît / <a href="mailto:bgaurier@ifremer.fr">bgaurier@ifremer.fr</a> Germain Grégory / <a href="mailto:ggermain@ifremer.fr">ggermain@ifremer.fr</a>	<b>Affiliation</b> PDG/REM/RDT/LCSM PDG/REM/RDT/LCSM PDG/REM/RDT/LCSM
<b>Encadrement(s) :</b>	
<b>Destinataire :</b>	
<b>Validé par :</b>	

# Contents

1	Experimental set-up	5
2	PIV database	8
3	Example of results	9
	References	9

# Introduction

Wake characterization takes an important part in tidal energy converters development. It is a requirement to design tidal energy converter arrays as it defines the optimal spacing between several devices. It is also used in environmental impact studies to assess potential modification of local currents and sediment transport.

The tidal energy converter studied here is based on the fluid-structure interactions that occur between a flexible membrane and an axial flow, resulting in an undulating motion that can be used to harvest energy. This device's performance has been studied [4] but its wake had never been quantified experimentally.

The wake of three experimental configurations are then studied here : a "free" configuration, with no PTO and a small pre-strain; an "intermediate" configuration, with PTO and small pre-strain; and an "efficient" configuration, with PTO and a greater pre-strain.

## 1 Experimental set-up

Experiments have been carried out in the Ifremer flume tank of Boulogne-sur-Mer (Fig. 1). Its working section is 18 m long, 4 m wide and 2 m deep. A window enables to film the membrane motion from the side in order to record its trajectory. Flow velocity is adjustable up to 2.2 m/s. Here, trials have been made at  $u_{\infty} = 1$  m/s with a mean upstream turbulence intensity rate of  $I_{\infty} = 1.5\%$  (Eq. 1). The turbulence intensity characterizes the level of fluctuations in the flow as a percentage, it is calculated here on two components.  $\sigma$  designates the standard deviation.

$$I_{2D} = 100 \sqrt{\frac{1}{2} \frac{\sigma(u')^2 + \sigma(v')^2}{\bar{u}^2 + \bar{v}^2}} \quad (1)$$

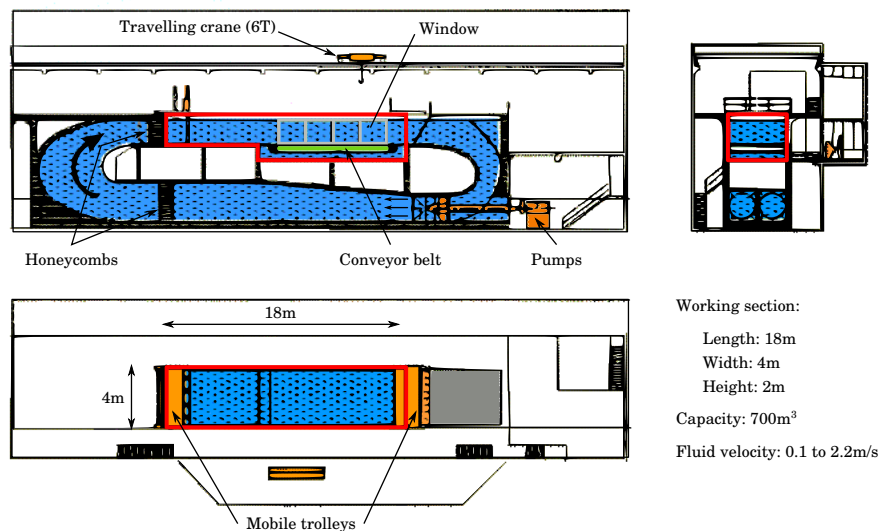


**Figure 1** – Schematic of the wave and current flume tank

The prototype used in the experiments is at  $1/20^{th}$  scale. It is made of a POM-C polyacetal membrane of dimensions  $L \times b \times h = 0.8 \text{ m} \times 0.8 \text{ m} \times 0.003 \text{ m}$ , density  $\rho = 1600 \text{ kg/m}^3$  and Young modulus  $E = 4.2 \text{ GPa}$  [4]. Blockage ratio is then about  $B = LA/(S_{canal}) \approx 0.04$ , with  $A$  the undulation amplitude.

This membrane is lengthened by  $0.15L$ -long rigid flaps at upstream and downstream extremities. In order to increase the transverse stiffness and to ensure a two-dimensional motion, six  $0.025L$ -wide carbon-epoxy bars

have been added in the transverse direction. They are separated by  $0.2L$  on the membrane and transmit forces to the converters through pivot fixations of height  $h_{fix} = 0.044L$  (Fig. 2).

To keep the structure in the middle of the water column, the membrane is clamped to a rigid vertical frame with three horizontal POM-C bars of dimensions  $0.250\text{ m} \times 0.046\text{ m} \times 0.010\text{ m}$ . The structure is also stressed by cables linking both extremities that keep the membrane bended (Fig. 2). The cables are shorter than the resting distance between their linking points. Their length is described through the cable withdraw length,  $d$ , as defined by Equation 2. Two withdraw length values will be considered in this paper: 7 % and 12.5 %.

$$d = \frac{L + L_{arm} - L_{cable}}{L} \quad (2)$$

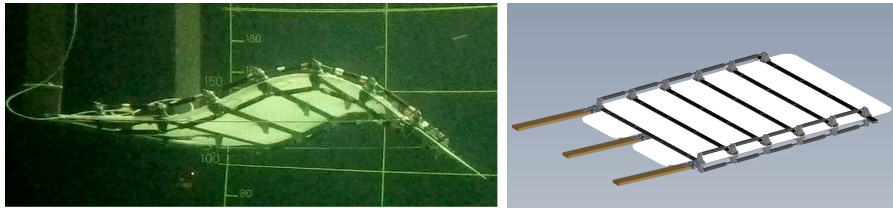


**Figure 2** – (a) Picture of  $1/20^{th}$  scale prototype during experiments in Ifremer flume tank of Boulogne-sur-Mer. (b) CAD 3D view of tested prototype. Membrane is in white, transverse bars in light grey, damper's fixation in dark grey and dampers in black.

At this scale, it is easier to dissipate energy than to convert it into electricity. Therefore, for physical and mechanical constraints, electromechanical converters are modeled by hydraulic dampers, as it has been experimented for oscillating body devices in wave converter models [1]. Four lines of 6 dampers are installed on the sides of the membrane, two above and two below (Fig. 2). The 24 dampers used in this study are the HB15/75/S/S/B from Slamproof Ltd, with a non-dimensional damping equal to  $C^* = 300$ .

$$C^* = C \frac{L^2 u_\infty}{EI_z} \quad (3)$$

The wake of three experimental configurations are studied : a "free" configuration, with no PTO and a small pre-strain, an "intermediate" configuration, with PTO and small pre-strain, and an "efficient" configuration, with PTO and a greater pre-strain. These configurations have been selected because they are close to the state-of-the-art efficient configuration that are used in the other studies on this device. Moreover, they have been selected to give an insight of the effect of damping and pre-strain on the wake dynamics, since these two parameters are the main adjustment parameters of the device. Furthermore, these three configurations have three different levels of extracted energy, the "free" configuration being closer to systems whose wake are studied in the existing literature. A summary of tested configurations is presented in Table 1. The undamped configuration is lighter because of the removal of dampers' weight.

Configuration	Mass	Dampers	Damping, $C^*$	Withdraw length, $d$
1	8.60 kg	none	0	7 %
2	10.1 kg	24	24x300	7 %
3	10.1 kg	24	24x300	12.5 %

**Table 1** – Summary of tested configurations.

In order to characterize the flow in the membrane's wake, measurements have been carried out by means of a 2D PIV system on a vertical plane along  $x$  and  $y$  axes and located at the middle of the membrane in the spanwise direction (Fig. 4). For these measurements, the tank has been seeded by silver-coated glass particles of diameter  $10\ \mu\text{m}$ . Illumination has been provided by a standard, frequency-doubled, double-cavity Nd:YAG Gemini-Like laser with up to 200 mJ per pulse using an excitation wavelength of 532 nm. The laser sheet is emitted in the



water by means of an optical system composed of cylindrical lenses mounted on a vertical laser-guiding arm in order to generate a light sheet on vertical plane. PIV images pairs are recorded at 15 Hz, with a low interval time of  $\Delta t = 1500 \mu s$  between the two frames of the pair [3]. The camera (Hi-sense CCD FlowSens EO-2M camera of  $1400 \text{ px} \times 900 \text{ px}$ ) is located perpendicularly to the laser sheet. The PIV system is synchronized with the motion tracking system through a trigger device. The distance between the camera and the laser sheet is 2.2 m, so that the PIV planes are located in the middle of the membrane in the transverse direction. Their dimensions are  $970 \text{ mm} \times 616 \text{ mm}$ . The uncertainty of the flow speed measured by PIV is estimated to be of 2.6% [2].

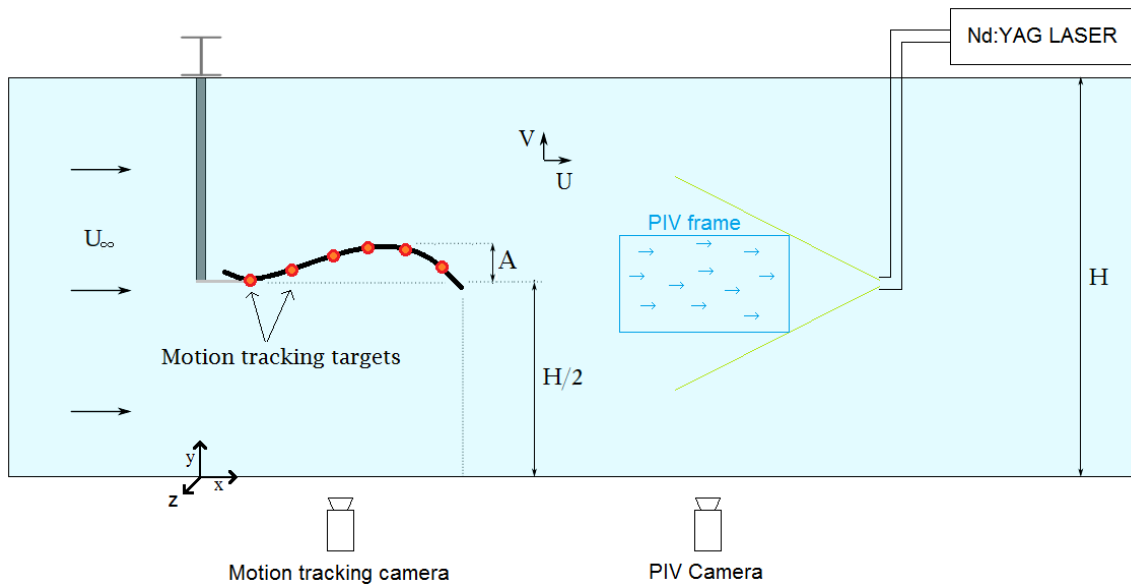


**Figure 3** – Drawing of the experiment instrumentation.

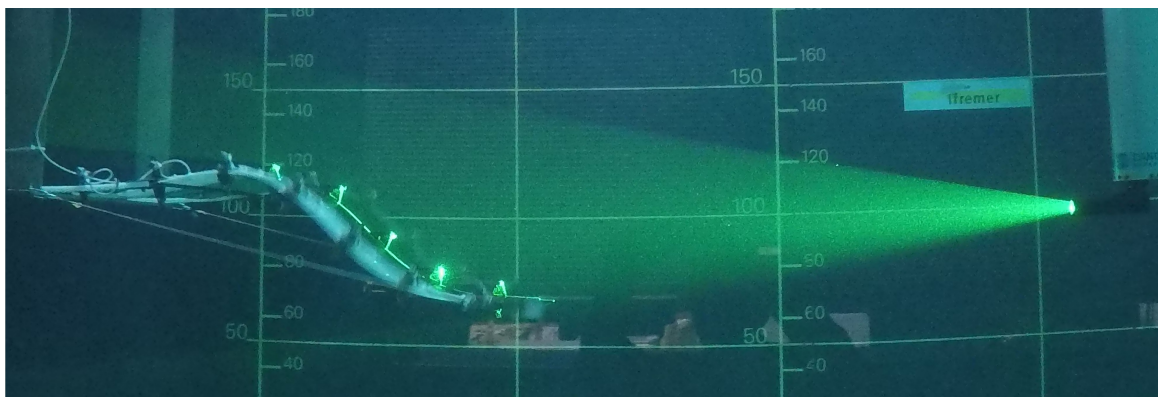


**Figure 4** – PIV measurements in the wake of the membrane.

## 2 PIV database

DynamicStudio software from Dantec Dynamics has been used for PIV image processing. Instantaneous velocity vector fields have been obtained using a single-pass cross-correlation algorithm with an interrogation window size of  $32 \text{ px} \times 32 \text{ px}$ , with 50% overlap. Streamwise ( $x$ -direction) and vertical ( $y$ -direction) velocity components are then available on a 2D regular mesh grid of  $(86 \times 55)$  points with an element length of 11.4 mm in each direction.

Universal Outlier Detection (UOD) algorithm is used to locate and replace abnormal vectors [5]. It detects those being different by a factor 2 of the mean value of the  $5 \times 5$  neighbor vectors. Abnormal vectors are then replaced by their neighbours' median value. Figure 5 summarizes the post-process stages on Dynamic Studio software.

The planes are registered one after the other so the post-process needs to put them back in space and time in order to generate global wake maps. Twenty-three planes have been registered during 300 s for each configuration, which enables to assemble planes on an area of  $2.25 \times 10L^2$ . However, on the sides of the planes, particles are not well lightened by the laser and there are some abnormal vectors. 3 px bands are then cut from analysis to remove them. Figure 6 presents the PIV planes layout with the tidal converter's trajectory superimposed.

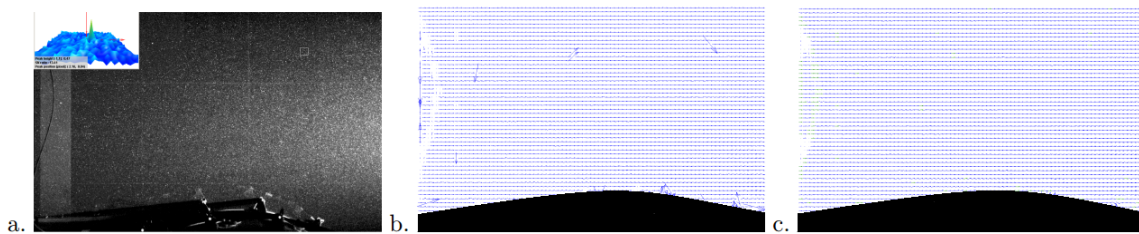


**Figure 5** – Post-processing stages on Dynamic Studio. (a) Raw image. (b) After cross-correlation algorithm. (c) After UOD algorithm.

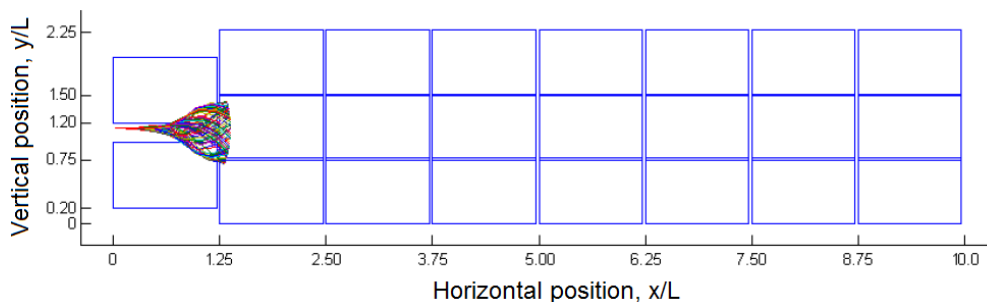


**Figure 6** – PIV planes location.

In order to synchronize every plane, motion tracking system is used to get the time step when the last target passes from below to above the membrane's fixation vertical position. As undulation frequency happens to vary, it is calculated in every plane and used to synchronize every period in order to calculate phase-averaged values. The uncertainty on the time a period starts is of the order of the sampling frequency inverse,  $1/f_e = 0.067 \text{ s}$ . Phase averages are then calculated with an uncertainty of the order of a hundredth of the undulation period.

The database is made of three matrices, one for each configuration. The matrices are presented as .mat files. In each matrix, one can find the synchronized axial and vertical flow speed,  $U$  and  $V$ , along with their horizontal and vertical position,  $X$  and  $Y$ .

### 3 Example of results

A way to quantify fluctuations levels in the flow is to calculate the turbulence intensity as shown in Figure 7. High level turbulence area seems to have a parabolic shape. The high turbulence intensity area ( $I_{2D} \geq 10\%$ ) fades away from  $x = 5L$  after the trailing edge. However, the area in the middle of the water column is much less impacted by the wake and low-level turbulence is there restored as soon as  $x = 3L$  after the trailing edge. It could then be a favourable area for a downstream tidal converter, assuming side effects have little influence and that membrane interaction is undesirable. Indeed, there is few fluctuations there.

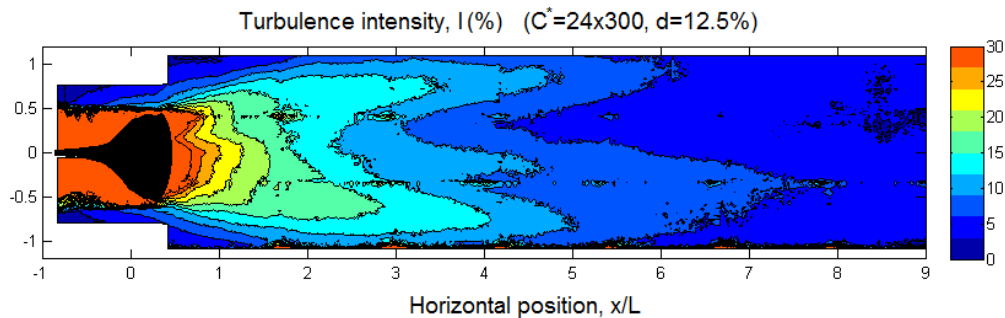


**Figure 7** – Mean turbulence intensity in the wake of the three tested configurations, C1 to C3 from top to bottom.

### Acknowledgment

This work was supported by the French Environment and Energy Management Agency (ADEME), Eel Energy SAS and the MET-CERTIFIED project, receiving funding from the Interreg 2 Seas programme 2014-2020, co-funded by the European Regional Development Fund under subsidy contract N° 2S01-020.

### References

- [1] A.H. Day et al. “Hydrodynamic modelling of marine renewable energy devices: A state of the art review.” In: *Ocean Engineering* 108 (2015), pp. 46–69.
- [2] M. Ikhennicheu, G. Germain, P. Druault, and B. Gaurier. “Experimental study of coherent flow structures past a wall-mounted square cylinder.” In: *Ocean Engineering* 182 (2019), pp. 137–146.
- [3] B. Mallat, G. Germain, B. Gaurier, P. Druault, and J-Y. Billard. “Experimental study of the bubble sweep-down phenomenon on three bow designs”. In: *Ocean Engineering* 148 (2018), pp. 361–375.
- [4] M. Träsch et al. “Power estimates of an undulating membrane tidal energy converter”. In: *Ocean Engineering* 148 (2018), pp. 115–124.
- [5] J. Westerweel and F. Scarano. “Universal outlier detection for PIV data”. In: *Experiments in Fluids* 39 (2005), pp. 1096–1100.